Dynamic nuclear polarization-enhanced solid-state NMR spectroscopy of GNNQQNY nanocrystals and amyloid fibrils

Galia T. Debelouchina,[†][a] **Marvin J. Bayro,**[†][a] **Patrick C. A. van der Wel,**[b]
Marc A. Caporini,[c] **Alexander B. Barnes,**[a] **Melanie Rosay,**[c]
Werner E. Maas[c] **and Robert G. Griffin***[a]

Dynamic nuclear polarization (DNP) utilizes the inherently larger polarization of electrons to enhance the sensitivity of conventional solid-state NMR experiments at low temperature. Recent advances in instrumentation development and sample preparation have transformed this field and have opened up new opportunities for its application to biological systems. Here, we present DNP-enhanced ^{13}C–^{13}C and ^{15}N–^{13}C correlation experiments on GNNQQNY nanocrystals and amyloid fibrils acquired at 9.4 T and 100 K and demonstrate that DNP can be used to obtain assignments and site-specific structural information very efficiently. We investigate the influence of temperature on the resolution, molecular conformation, structural integrity and dynamics in these two systems. In addition, we assess the low-temperature performance of two commonly used solid-state NMR experiments, proton-driven spin diffusion (PDSD) and transferred echo double resonance (TEDOR), and discuss their potential as tools for measurement of structurally relevant distances at low temperature in combination with DNP.

Introduction

In recent years, dynamic nuclear polarization (DNP) has gained ground as a highly promising method to increase the sensitivity of MAS solid-state NMR experiments.[1,2] The technique utilizes the inherently larger polarization of electrons that are introduced in the sample in the form of a biradical, typically TOTAPOL.[3,4] The biradical's EPR spectrum is irradiated with microwaves at cryogenic temperatures and the electron polarization is transferred to the ^1H nuclei *via* the cross effect.[5–7] This is a three-spin mechanism that involves a spin flip-flop process of the two dipolar coupled electrons in the biradical and the generation of ^1H nuclear polarization when the following matching condition is satisfied $\omega_{0s1} - \omega_{0s2} = \omega_{0I}$, where ω_{0s1}, ω_{0s2} and ω_{0I} are the Larmor frequencies of the two electrons and the ^1H spin respectively. The theoretical enhancement for ^1H nuclei is ~ 660, while experimental enhancements on the order of 250 at 5 T and 100 at 9.0 T have been achieved.[8,9]

Recent advances in instrumentation such as stable low-temperature MAS probes with sample insert/eject systems,[8,10] reliable high-field microwave sources (gyrotrons)[11,12] and improved cryogenic technology[13] have transformed the field of DNP and have placed the routine collection of multidimensional

correlation experiments on various biological systems within reach.[14,15] Here, we present DNP-enhanced ^{13}C–^{13}C and ^{15}N-^{13}C correlation experiments on GNNQQNY nanocrystals and amyloid fibrils acquired at 9.4 T and 100 K and demonstrate that DNP can be used to obtain assignments and site-specific structural information very efficiently.

GNNQQNY nanocrystals have previously been used as a model system to demonstrate the transfer of DNP-enhanced ^1H polarization across a glassy matrix–crystal interface at 5 T.[16] This seven-residue fragment can form two types of crystals (monoclinic and orthorhombic) and their crystal structures reveal the presence of the typical amyloid "cross-beta" motif and a steric zipper that was suggested to be the basis of amyloid fibrils in general.[17,18] The steric zipper forms a dry interface while a network of water molecules forms a 0.7 nm wide channel that comprises the wet interface. TOTAPOL is too large to reside inside the water channel, and it was shown that it does not interact with the bulk molecules inside the monoclinic crystals.[16] ^1H–^1H spin diffusion, however, successfully transfers the polarization through the crystal interface and leads to an enhancement of ~ 120 at 5 T. Although this enhancement allowed the rapid acquisition of a two-dimensional ^{13}C–^{13}C correlation spectrum, the low magnetic field limited the spectral resolution and precluded the assignment of the resonances in the crystals.

Under slightly different experimental conditions, GNNQQNY can also form amyloid fibrils. ^{13}C–^{13}C and ^{15}N–^{13}C MAS spectra of these fibrils reveal the presence of three distinct conformational subsets that differ from the crystals both in their chemical shifts and the mobility of the side chains.[19] One of these forms, in particular, exhibits significant non-β sheet

[a] Department of Chemistry and Francis Bitter Magnet Laboratory, Massachusetts Institute of Technology, Cambridge, MA 02139, USA. E-mail: rgg@mit.edu; Tel: +1 617 253 5405
[b] Department of Structural Biology, University of Pittsburgh School of Medicine, Pittsburgh, PA 15260, USA
[c] Bruker BioSpin Corp, Billerica, MA 01821, USA
† These authors contributed equally to the presented work.

character, which raises interesting questions regarding the fibril architecture. Obtaining long-range distances that could potentially establish the intermolecular arrangement in the fibrils, however, presents a significant challenge in this relatively small system due to the very degenerate amino acid composition and the multiplicity exhibited in the solid-state NMR spectra.

Here, we use DNP-enhanced ^{13}C–^{13}C and ^{15}N–^{13}C MAS correlation spectra of GNNQQNY monoclinic crystals and fibrils to obtain resonance assignments of the two systems at 100 K. The low-temperature behavior of each system can be affected by a variety of factors including, but not limited to, changes in the internal dynamics of the peptide backbone and side chains, structural rearrangements due to interactions with the solvent, and freezing-out of disordered or heterogeneous regions of the molecule. These factors can lead to significant deviations in the chemical shifts compared to room temperature and can have profound effects on the linewidths and resolution observed in the DNP-enhanced low-temperature spectra. Furthermore, we compare the performance of two commonly used solid-state NMR experiments, PDSD[20] and TEDOR,[21,22] to room-temperature data and discuss their potential as tools for measurement of structurally relevant distances at low temperature in combination with DNP.

Experimental

Sample preparation

Monoclinic crystals of 100% [U–^{13}C,^{15}N GNNQ]QNY and amyloid fibrils of 100% GNN[U–^{13}C,^{15}N QQN]Y peptide (New England Peptide, Gardner, MA) were obtained by following the previously described protocol.[19,23] The crystals were suspended in a 70/23/7% (w/w/w) glycerol–d_8/D_2O/H_2O matrix containing 35 mM TOTAPOL[4] and centrifuged directly into a 3.2 mm Bruker sapphire rotor using a tabletop centrifuge (16 000 × g). The fibrils were placed in a 70/23/7% (w/w/w) glycerol–d_8/D_2O/H_2O matrix containing 10 mM TOTAPOL and pelleted at 265 000 × g. The pellet was subsequently transferred into the rotor using a tabletop centrifuge. The [U–^{13}C,^{15}N GNNQ]QNY monoclinic crystal sample will be referred to as "GNNQqny" in the following sections, while the GNN[U–^{13}C,^{15}N QQN]Y fibrils will be abbreviated as "gnnQQNy". The labeling of the residues in the peptide follows the nomenclature used in ref. 19 and the fibril forms a, b and c in this work correspond to published forms #1, 2 and 3 respectively.[19] ^{13}C chemical shifts were referenced to aqueous DSS[24], while ^{15}N chemical shifts were referenced indirectly to liquid NH_3.[25,26]

DNP experiments

DNP experiments were performed on a Bruker 263 GHz Solids DNP spectrometer, consisting of a 263 GHz continuous-wave gyrotron source, microwave transmission line, 3.2 mm low-temperature (100 K) MAS probe, gas cooling supply, and 400 MHz AVANCE III wide-bore NMR system.[10] 2.5 μs ^1H, 4.5 μs ^{13}C and 5.0 μs ^{15}N $\pi/2$ pulses were used for the CP experiments and the PDSD[20] and TEDOR[22] correlations described below. 100 kHz ^1H decoupling was used during

the acquisition, evolution and TEDOR mixing periods. The recycle delay was set to 6 s for the crystal sample, and 6.5 s for the fibril sample. Each TEDOR experiment was acquired with 32 scans per t_1 point, 96 t_1 points and dwell time of 111 μs (∼5 h for the crystals and ∼5.5 h for the fibrils). The PDSD experiments were acquired with four scans per t_1 point, 384 t_1 points, and a dwell time of 56 μs (∼3 h each).

300 K Experiments

Room-temperature experiments were performed on custom-designed spectrometers (courtesy of D. J. Ruben, Francis Bitter Magnet Laboratory, Massachusetts Institute of Technology, Cambridge, MA) operating at 750 and 700 MHz ^1H Larmor frequency. The 750 MHz spectrometer was equipped with a 3.2 mm triple-resonance ^1H/^{13}C/^{15}N Bruker E^{free} probe (Billerica, MA), and the 700 MHz experiments were performed on a 3.2 mm triple-resonance Varian Chemagnetics probe (Palo Alto, CA). The sample temperature during the MAS experiments was estimated to be ∼300 K. The recycle delay was set to 3 s for all experiments at this temperature. A 2D TEDOR experiment was collected with the fibril sample at 750 MHz, $\omega_r/2\pi$ = 9 kHz, τ_{mix} = 1.8 ms, 128 scans per t_1 point, 96 t_1 points and dwell time of 111 μs (∼10 h). A PDSD experiment was collected with τ_{mix} = 10 ms, 28 scans per t_1 point, 668 t_1 points, and dwell time of 24 μs (∼16 h). Due to low S/N we did not record 2D TEDOR experiments with the crystal sample.

Results and discussion

DNP of GNNQqny monoclinic crystals

A typical DNP-enhanced 1D ^{13}C CP spectrum of the GNNQqny crystals is presented in Fig. 1 and compared to a spectrum obtained without simultaneous microwave irradiation. The enhancement due to DNP varies for the different components of the sample, i.e. the enhancement for the two glycerol peaks at ∼70 ppm is ∼40, while the enhancement observed for the signals arising from the peptide is ∼20. The explanation for this behavior is that TOTAPOL remains outside the crystals and the polarization has to cross the barrier between the glassy solvent and the crystal interior.[16]
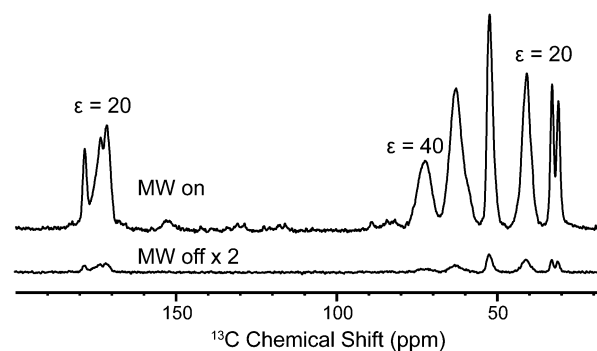

Fig. 1 ^{13}C CP spectra of [U–^{13}C,^{15}N GNNQ]QNY monoclinic crystals recorded with (top) and without (bottom) DNP. The enhancement for the signals arising from the crystals is ∼20, while the enhancement for the glycerol peaks is ∼40. The MW irradiation time is 6 s for both spectra.
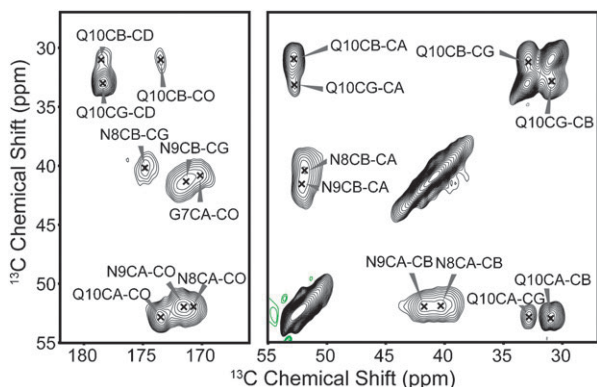
Fig. 2 DNP-enhanced ^{13}C–^{13}C PDSD correlation spectrum of [U–^{13}C,^{15}N GNNQ]QNY monoclinic crystals obtained at 9.4 T, 105 K, $\omega_r/2\pi = 9$ kHz, and $\tau_{mix} = 5$ ms.

This is also manifested by the slower rate of polarization build-up for the peptide residues (10–12 s for the peptide vs. 3 s for glycerol).

The fact that TOTAPOL remains excluded from the crystals offers some significant advantages. First, the concentration of TOTAPOL can be increased quite significantly without compromising the linewidth of the spectra. It has been demonstrated that concentrations up to 70 mM in the crystal samples do not lead to significant line broadening at room temperature.[16] Using a higher radical concentration allows for much faster polarization times and scan delays and significantly improves the signal-to-noise (S/N) ratio per unit time.[27] Second, the spectroscopic behavior of the bulk of the peptide molecules can be expected to be only modestly influenced by the presence of radical electrons in the sample, resulting in relaxation parameters that are predominantly governed by temperature and less by the electron–nuclear interaction.

The enhancement due to the cross effect is inversely proportional to the field,[28] and therefore the expected enhancement at 9.4 T would be 1.9 times smaller than the enhancement reported at 5 T. However, the field alone does not explain why the observed enhancement in this study is ~ 20 for the peptide resonances instead of the expected 63. Differences in the experimental conditions, in particular the higher temperature used to record the current data set, are probably significant contributing factors to the lower enhancement. An important observation, however, is that at 100 K, the sensitivity enhancement just due to the temperature effect is ~ 5 (data not shown) as a result of the larger spin polarization and the improved efficiency of the probe at low temperature. Therefore, the overall enhancement compared to 300 K is ~ 100, resulting in significant gains in the time necessary to record correlation experiments.

Assignments of the four labeled residues were obtained through a ^{13}C–^{13}C correlation experiment recorded with PDSD mixing ($\tau_{mix} = 5$ ms) (Fig. 2) and one- and two-bond ^{15}N–^{13}C correlation experiments recorded with TEDOR mixing[21,22] (Fig. 3). These spectra present improved resolution compared to previously published spectra at 5 T,[16] and despite the heterogeneity and large linewidths observed for some sites, the complete low-temperature assignment of all the labeled resonances in the crystals was possible.

The TEDOR spectrum of the crystals presented in Fig. 3 and recorded with $\tau_{mix} = 3.6$ ms is of particular interest as it shows two cross-peaks consistent with intermolecular contacts between Q10NE2 and N9CA and Q10NE2 and Q10CA respectively (Fig. 4) with interatomic distances that correspond to ~ 4 Å. In a uniformly labeled sample, the typical one-bond (1.2 Å) transfer efficiency is $\sim 25\%$, while for a concurrent 4 Å distance, the efficiency is reduced to 2%.[22] Gln and Asn residues, in particular, contain multiple strong and
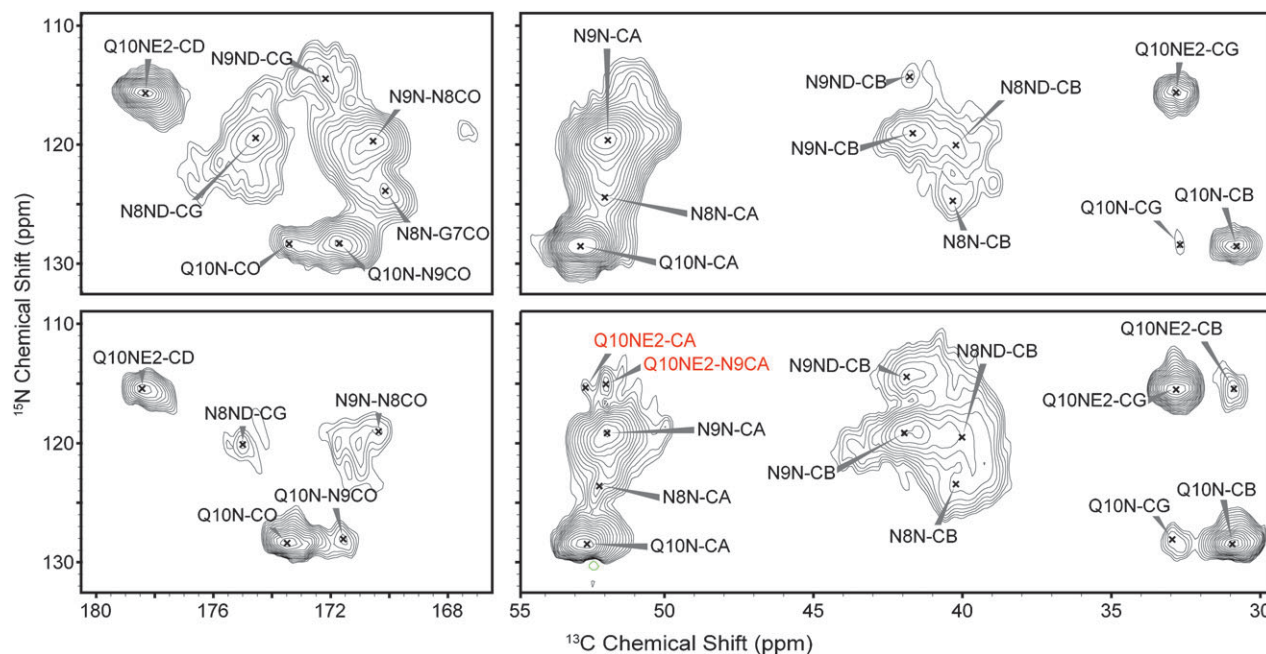

Fig. 3 DNP-enhanced TEDOR spectra of [U–^{13}C,^{15}N GNNQ]QNY monoclinic crystals obtained at 9.4 T, 105 K, $\omega_r/2\pi = 9$ kHz, and $\tau_{mix} = 1.8$ ms (top), and 3.6 ms (bottom). Two intermolecular contacts are observed at $\tau_{mix} = 3.6$ ms.
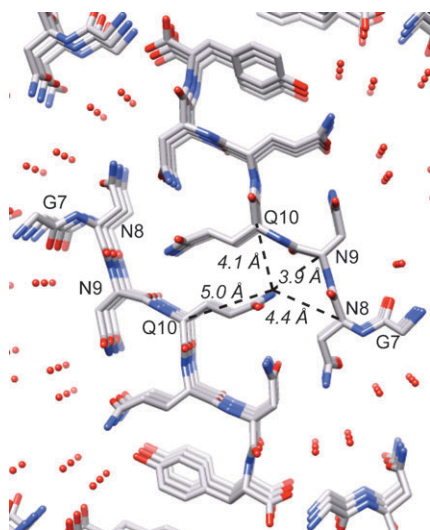
Fig. 4 Crystal lattice of monoclinic GNNQQNY (PDB ID 1YJP).[17] Several possible intra- and intermolecular contacts between Q10 NE and the CA atoms of other labeled residues are indicated. The image was produced using the Chimera software.[29]

medium ^{15}N–^{13}C dipolar couplings that further complicate the transfer between weakly coupled nuclei like the intermolecular contacts shown here. The measurement of such structurally relevant distances is therefore quite difficult and very often also complicated by the presence of dynamics at room temperature. The DNP-enhanced TEDOR spectra, however, demonstrate that such important structural information can be recorded with sufficient intensity at low temperature in cases where enough resolution is available.

DNP of gnnQQNy fibrils

Solid-state MAS NMR spectra of gnnQQNy amyloid fibrils exhibited a DNP enhancement factor of 35, as shown in Fig. 5a. Unlike the case of the crystals, the glycerol resonances in the ^{13}C CP spectra are enhanced by an identical factor to the fibril resonances. In addition, fibril and solvent signals present similar polarization build-up rates (5 s for the fibrils, and 5.5 s for glycerol). This behavior indicates that the biradical molecules, dispersed in the glycerol/water solvent matrix, are likely to be also in intimate contact with the fibril molecules. The small width of the fibrils (a few nanometres in their thinnest dimension)[19] allows close contact between the para-magnetic centers and a large fraction of the peptide molecules. Furthermore, enhanced ^{1}H polarization is spread *via* spin diffusion and may equilibrate rapidly throughout the fibril. Indeed, rapid polarization equilibration *via* spin diffusion is likely to be the reason why the DNP enhancement factor for the fibrils is considerably larger than for the much thicker crystals, despite a lower radical concentration in the fibrils (10 mM) than in the crystals (35 mM). The lower radical con-centration, however, leads to the slightly lower enhancement observed for the glycerol resonances and their longer polariza-tion build-up time.

Given the apparent close proximity between paramagnetic centers and fibril molecules, it is remarkable that high-magnetic-field spectra of gnnQQNy fibrils prepared with (Fig. 5b) and

without biradicals (Fig. 5c) are equally well resolved, demon-strating that the resonance broadening effect of TOTAPOL biradicals at this concentration (10 mM) is marginal for these fibril samples. In addition, the room-temperature spectrum in Fig. 5b was recorded on the same sample as that in Fig. 5a after performing our DNP experiments at 100 K. Since both room-temperature spectra (Fig. 5b and c) present virtually no chemical shift discrepancies, it is evident that the fibrils experience little damage as a result of the low temperatures, likely due to adequate cryoprotection by the glycerol–water solvent. While it is clear that 400 MHz spectra recorded at 100 K with DNP present significantly larger linewidths than those of 750 MHz spectra recorded at room temperature, chemical shift variations are very small, as described in detail below, which indicates that the fibrils preserve their integrity while at low temperatures.

Homonuclear correlation spectra of gnnQQNy fibrils recorded with PDSD mixing present strong cross-peaks with multiple resolved ^{13}C sites. Fig. 6 compares a 2D PDSD spectrum recorded at 750 MHz and 300 K without DNP (Fig. 6a) to one recorded at 400 MHz and 100 K with DNP (Fig. 6b). The linewidth differences observable in 1D spectra are more conspicuous here. For example, the ^{13}C linewidths for the resolved N12 cross-peaks at room temperature are 0.8–1 ppm, while they are 1.3–1.75 ppm at 100 K. On the other hand, the DNP-enhanced spectrum presents a number of resolved sites and allows the identification of various spin systems without referring to data at room temperature. For example, one of the fibril forms, here referred to as "form a", has been completely assigned, while the three different forms of N12 are easy to identify.

Longitudinal mixing efficiency appears to improve at low temperature, as evidenced by increased cross-peak intensities. In addition, polarization transfer appears to occur at a faster rate at 100 K, with two-bond correlations appearing strongly after 5 ms of mixing while they are still relatively weak after 10 ms of mixing at room temperature. Such dynamic effects manifested as a low-temperature enhancement in mixing efficiency are advantageous from a practical perspective, but they might also be critical in the study of complex biomolecules that exhibit extensive dynamics. For example, form b of GNNQQNY fibrils appears to be more dynamic than forms a and c at room temperature, as evidenced by the lower CP signal intensity for residue N12 of form b (Fig. 5b and c), and ^{13}C and ^{15}N relaxation experiments.[30] The cross-peak corres-ponding to N12b CA-CO is at the noise level in the room-temperature spectrum (Fig. 6a) while other N12b cross-peaks do appear, indicating a degree of dynamic disorder. On the other hand N12b CA-CO is observed with sufficient intensity in the DNP-enhanced PDSD spectrum at 100 K (Fig. 6b).

The influence of temperature on the dynamics of the fibrils is also readily observed in heteronuclear correlation spectra. The TEDOR spectra presented in Fig. 7 depict several well-resolved ^{15}N–^{13}C correlations at 750 MHz and room tempera-ture (Fig. 7a) and at 400 MHz and 100 K with DNP (Fig. 7b and c). TEDOR recorded with τ_{mix} = 1.8 ms is optimal for one-bond heteronuclear correlations, corresponding in gnnQQNy to five backbone (three N_i-CA_i and two N_i-CO_{i-1}) and three side-chain contacts for each of the three forms of fibrils.

5914 | *Phys. Chem. Chem. Phys.*, 2010, **12**, 5911–5919

This journal is © the Owner Societies 2010

a)

ε = 35

ε = 35

MW on

ε = 35

*

MW off

150   100   50
^{13}C Chemical Shift (ppm)

b)

*   *

150   100   50
^{13}C Chemical Shift (ppm)

c)

*   *

150   100   50
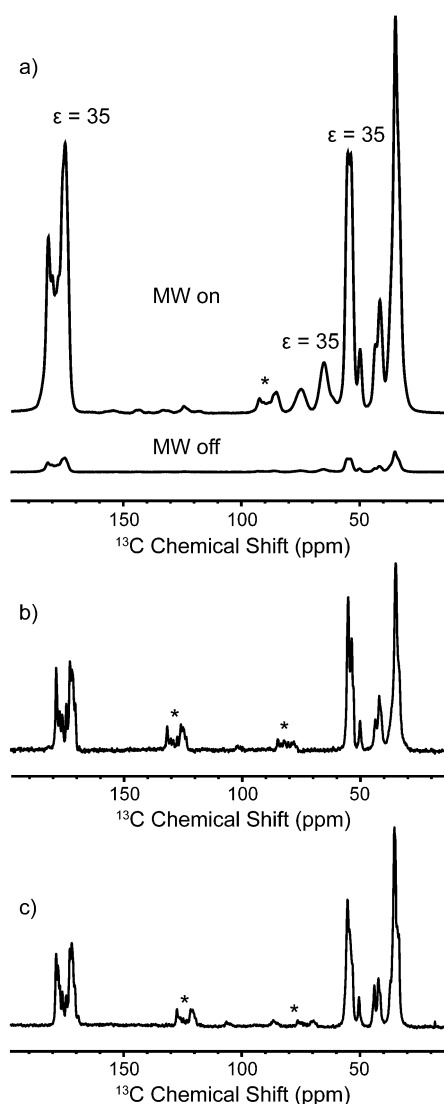^{13}C Chemical Shift (ppm)

Fig. 5 (a) ^{13}C CP spectra of GNN[U–^{13}C,^{15}N QQN]Y fibrils obtained with DNP (top) and without DNP (bottom) at 400 MHz, $\omega_r/2\pi$ = 9 kHz, 100 K, 16 scans, and MW irradiation time of 6.5 s. The enhancement for the fibrils and the glycerol peaks is 35. (b) ^{13}C CP spectrum obtained with the same sample after the DNP experiments were performed. Spectrum was recorded at 750 MHz. (c) ^{13}C CP spectrum of fibrils prepared without radical and glycerol, recorded at 700 MHz. Experimental parameters for (b) and (c) are $\omega_r/2\pi$ = 9 kHz, 300 K, 128 scans, and scan delay of 3 s. Asterisks denote side bands.

Fig. 6 ^{13}C–^{13}C correlations of GNN[U–^{13}C,^{15}N QQN]Y fibrils collected at (a) 750 MHz without DNP, PDSD τ_{mix} = 10 ms, $\omega_r/2\pi$ = 9 kHz, 300 K, and (b) 400 MHz with DNP, PDSD τ_{mix} = 5 ms, $\omega_r/2\pi$ = 9 kHz, 100 K. The asterisks in (a) denote side bands.

At this short mixing time, the room temperature spectrum presents almost exclusively one-bond correlations, with two-bond contacts slightly above the noise level. On the other hand, the low-temperature, DNP-enhanced 1.8 ms TEDOR spectrum of Fig. 7b, presents very intense two-bond ^{15}N–^{13}C correlations in addition to the expected one-bond contacts. The overall sensitivity of the DNP-enhanced TEDOR spectrum is excellent, given that in addition to the polarization enhancement factor, the recoupling efficiency itself at low temperature is comparable or superior to that at room temperature. Increasing the mixing time allows the build-up of two-bond correlations, shown at their approximate maximum in Fig. 7c, which was recorded with τ_{mix} = 3.6 ms.
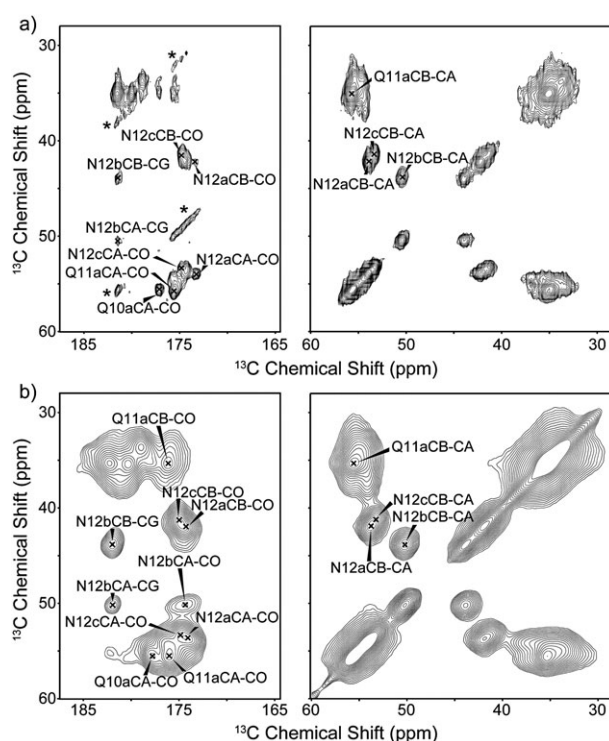
We recorded several 2D DNP-enhanced TEDOR spectra of gnnQQNy fibrils with τ_{mix} ranging from 0.9 ms to 7.2 ms, from which several build-up curves were extracted, plotted in Fig. 8a. Comparison of ^{13}C signals after CP and after TEDOR with a short mixing time in 1D allows us to evaluate the efficiency of one-bond recoupling. The corresponding cross-peaks in 2D spectra can then be compared to other cross-peaks to obtain an estimate of their recoupling efficiency, taking into account the original CP intensity of the nuclei involved. One-bond transfer efficiencies were ∼20%, while efficiencies around 7% were obtained for two-bond transfers. These numbers are comparable to theoretical values, however, it is apparent in Fig. 8a that the two-bond build-up curves decay somewhat quickly, after 4–5 ms, which is consistent with rapid transverse relaxation. Indeed, ^{13}C echo experiments at 100 K with high-power ^{1}H decoupling show T'_2 times of ∼5 ms for the fibrils. Since the TEDOR pulse sequence contains two echo segments in the ^{13}C channel during the ^{15}N–^{13}C recoupling period, significant polarization losses can be expected at increasing mixing times.

As a comparison to our DNP-enhanced, low-temperature TEDOR build-up curves, we recorded similar curves at room temperature, shown in Fig. 8b. Due to the low signal-to-noise ratio without DNP, we recorded the room-temperature profiles in 1D fashion. A few interesting differences are readily observed. First, the decay of CA magnetization is much slower than at 100 K, consistent with reduced relaxation processes for the fibrils at room temperature. The decay of ^{13}C signals after

Fig. 7 ^{15}N–^{13}C correlation experiments of GNN[U–^{13}C,^{15}N QQN]Y fibrils recorded with TEDOR mixing. (a) Spectrum recorded at 750 MHz, $\omega_r/2\pi$ = 9 kHz, 300 K and τ_{mix} = 1.8 ms. (b) and (c) Spectra recorded with DNP at 400 MHz, $\omega_r/2\pi$ = 9 kHz, 100 K and τ_{mix} = 1.8 ms and 3.6 ms respectively.

Fig. 8 1D TEDOR build-up curves of GNN[U–^{13}C,^{15}N QQN]Y fibrils obtained at (a) 400 MHz, 100 K with DNP and (b) 750 MHz, 300 K, without DNP.

5916 | *Phys. Chem. Chem. Phys.*, 2010, **12**, 5911–5919

This journal is © the Owner Societies 2010

polarization build-up in a TEDOR experiment is driven by both relaxation and the strength of the effective ^{15}N–^{13}C couplings. The increased dynamics at room temperature, however, may also be responsible for a decreased recoupling efficiency for two-bond contacts (2.5 to 4%) compared to low-temperature data (7%). A third noteworthy difference is that while ^{13}C nuclei with the same ^{15}N–^{13}C coupling strength (one- or two-bond) have similar TEDOR profiles at low temperature, they vary considerably at room temperature. These observations suggest that measuring internuclear distances at low temperatures with experiments such as TEDOR (and DNP) may have significant advantages over room-temperature experiments.

Temperature-dependent structural changes

The experiments described above have allowed us to assign all labeled residues in GNNQqny monoclinic crystals and a significant number of the cross-peaks for gnnQQNy fibrils at 100 K. The obtained chemical shifts, together with the line-width exhibited in the spectra, provide important information regarding the structural rearrangements and the changes in dynamics the two samples undergo upon freezing. While the change in temperature seems to have little effect on the structural integrity and conformational stability of the fibrils, it affects the residues in the crystals more profoundly.

Comparison of the published room-temperature chemical shifts[19] (300 K) and the low-temperature chemical shifts presented here (100 K) for GNNQqny monoclinic crystals reveals significant structural changes for some of the residues. In particular, the ^{13}C chemical shifts for most sites in G7, N8 and N9 differ by more than 1 ppm between 100 K and 300 K, while the difference for the ^{15}N chemical shifts can be as much as 5 ppm (Fig. 9). The corresponding differences for Q10, however, are less dramatic. Closer inspection of the spectra presented in Fig. 2 and 3 also indicates that the cross-peaks that have been assigned to the glutamine spin system exhibit narrower line widths (ca. 1.1–1.75 ppm for ^{13}C resonances and 1.8–2.5 ppm for ^{15}N resonances) and a much lower degree of heterogeneity. In comparison, the linewidth of the N8CB-CA cross-peak in the PDSD spectrum (Fig. 2) is ~1.8 ppm in the direct dimension, while the N9N-CA cross-peak in Fig. 3 is ~1.6 ppm for ^{13}C and ~3 ppm for ^{15}N.

Residue Q10 plays an important role in the intermolecular interactions of GNNQQNY monoclinic crystals, as it is tightly locked in the dry "steric zipper" that forms between the β-sheets in the crystals (Fig. 4). The other three residues labeled in this study, however, are in intimate contact with the crystallographic water. Water molecules are found to be an integral part of many protein crystal structures, where they may have a key structural or functional role. Despite their ubiquitous presence, however, there have been few reports documenting their influence on the dynamics of the groups they interact with in protein crystals.[31–36] At room temperature, these studies are also complicated by the exchange between crystallographic water and the bulk solvent water, as well as chemical exchange between labile protein protons and water molecules in general. Although the effect of temperature on the dynamic behavior of the crystallographic water molecules is not well
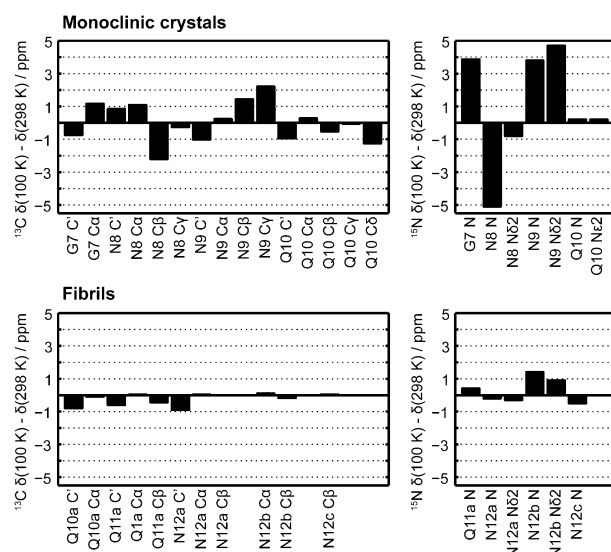

Fig. 9 Comparison of the ^{13}C and ^{15}N chemical shifts obtained at 100 K with DNP and 298 K without DNP for [U–^{13}C,^{15}N GNNQ]QNY monoclinic crystals (top) and GNN[U–^{13}C,^{15}N QQN]Y fibrils (bottom).

understood, it is highly probable that as the sample freezes they undergo structural rearrangements that are translated to the neighboring atoms via non-specific interactions and lead to both the chemical shift displacement and the increase in line-width and heterogeneity observed here. The room-temperature spectra of the crystals[19] show no significant differences in the dynamics of the different residues (as evidenced by their similar cross-peak intensities and linewidth), implying that the freezing-out of different conformations accessible at room temperature due to inherent dynamics of the peptide is not likely.

The effect of the freezing of the bulk solvent, on the other hand, is lessened by the glycerol co-solvent, a popular cryoprotectant that was also used for the X-ray crystallography studies of the monoclinic crystals.[17] In glycerol–water mixtures, glycerol is thought to disrupt the hydrogen-bonding network of the bulk water molecules and to prevent detrimental ice formation upon freezing.[37,38] The impact of the solvent water molecules on the linewidth observed in the spectra should also be limited by the high concentration of radical close to the crystal surface that may effectively suppress the broadened signals from the surface exposed peptides.

Remarkably, temperature seems to have a less significant impact on the chemical shifts of the gnnQQNy fibrils (Fig. 9). The changes in the chemical shifts of the assigned residues are <1 ppm for ^{13}C, and <1.5 ppm for ^{15}N, much smaller than the dramatic chemical shifts differences observed for some sites in the crystals. While the linewidths are slightly broader than those observed at room temperature, there are no particular patterns that indicate that certain sites exhibit more line broadening than others at low temperature. This observation, combined with the room-temperature control experiments shown in Fig. 5, imply that the effects of lowering the temperature are more uniform and reversible in the fibril sample and much more significant than the effect of the biradical. Future work on cryoprotection might help reduce

the linewidth further at 100 K, which would not only facilitate the assignment process of the spectra, but would also increase T'_2 values so that the efficiency of experiments like TEDOR could be improved for the longer distance spin pairs.

Conclusions

Here, we present DNP-enhanced solid-state NMR data of GNNQQNY nanocrystals and amyloid fibrils obtained at 100 K and 9.4 T. DNP leads to significant enhancements in the signal-to-noise ratio (20 for the nanocrystals and 35 for the fibril sample), allowing the acquisition of two-dimensional correlation spectra with great time efficiency. The higher magnetic field utilized in this study has allowed us to record well-resolved low-temperature PDSD and TEDOR spectra and to obtain assignments for all labeled residues in the crystal sample and for a large number of the labeled sites in the fibrils. Chemical shift and linewidth comparison to room-temperature data indicates that the residues in close contact to the water molecules in the crystals undergo profound structural changes that can lead to inhomogeneous broadening. While little can be done in such cases where the sources of line broadening are inherent to the system, more work is necessary to understand the temperature response of these systems. In the fibril case, on the other hand, the chemical shifts change very little with temperature and while the linewidths increase uniformly by 40–60 Hz, this process is reversible. Work with other fibril systems is currently in progress to assess the generality of this behavior.

The enhanced sensitivity due to DNP, combined with diminished dynamic processes at low temperature that could otherwise interfere with recoupling efficiency, lead to PDSD and TEDOR correlation spectra that are much richer in information content. This is especially the case for shorter mixing times where relaxation losses are less pronounced. Improvements in the sample preparation technique and cryo-protection could lead to samples with enhanced resolution and relaxation properties. Such developments will undoubtedly open new avenues for the application of DNP in biomolecular solid-state NMR.

Acknowledgements

References

1 T. Maly, G. T. Debelouchina, V. S. Bajaj, K.-N. Hu, C.-G. Joo, M. L. Mak-Jurkauskas, J. R. Sirigiri, P. C. A. van der Wel, J. Herzfeld, R. J. Temkin and R. G. Griffin, *J. Chem. Phys.*, 2008, **128**, 052211.
2 A. B. Barnes, G. De Paepe, P. C. A. van der Wel, K. N. Hu, C. G. Joo, V. S. Bajaj, M. L. Mak-Jurkauskas, J. R. Sirigiri, J. Herzfeld, R. J. Temkin and R. G. Griffin, *Appl. Magn. Reson.*, 2008, **34**, 237.
3 K. N. Hu, C. Song, H. Yu, T. M. Swager and R. G. Griffin, *J. Chem. Phys.*, 2008, **128**, 052302.
4 C. Song, K. N. Hu, C. G. Joo, T. M. Swager and R. G. Griffin, *J. Am. Chem. Soc.*, 2006, **128**, 11385.
5 A. V. Kessenikh, A. A. Manenkov and G. I. Pyatnitskii, *Phys. Solid State*, 1964, **6**, 641.
6 C. F. Hwang and D. A. Hill, *Phys. Rev. Lett.*, 1967, **19**, 1011.
7 D. S. Wollan, *Phys. Rev. B: Solid State*, 1976, **13**, 3671.
8 A. B. Barnes, M. L. Mak-Jurkauskas, Y. Matsuki, V. S. Bajaj, P. C. A. van der Wel, R. DeRocher, J. Bryant, J. R. Sirigiri, R. J. Temkin, J. Lugtenburg, J. Herzfeld and R. G. Griffin, *J. Magn. Reson.*, 2009, **198**, 261.
9 Y. Matsuki, T. Maly, O. Ouari, H. Karoui, F. Le Moigne, E. Rizzato, S. Lyubenova, J. Herzfeld, T. Prisner, P. Tordo and R. G. Griffin, *Angew. Chem., Int. Ed.*, 2009, **48**, 4996.
10 M. Rosay, L. Tometich, S. Pawsey, R. Bader, R. Schauwecker, M. Blank, P. M. Borchard, S. R. Cauffman, K. L. Felch, R. T. Weber, R. J. Temkin, R. G. Griffin and W. E. Maas, *Phys. Chem. Chem. Phys.*, 2010, **12**, DOI: 10.1039/c003685b.
11 V. S. Bajaj, C. T. Farrar, M. K. Hornstein, I. Mastovsky, J. Vieregg, J. Bryant, B. Elena, K. E. Kreischer, R. J. Temkin and R. G. Griffin, *J. Magn. Reson.*, 2003, **160**, 85.
12 V. S. Bajaj, M. K. Hornstein, K. E. Kreischer, J. R. Sirigiri, P. P. Woskov, M. L. Mak-Jurkauskas, J. Herzfeld, R. J. Temkin and R. G. Griffin, *J. Magn. Reson.*, 2007, **189**, 251.
13 P. J. Allen, F. Creuzet, H. J. M. De Groot and R. G. Griffin, *J. Magn. Reson.*, 1991, **92**, 614.
14 V. S. Bajaj, M. L. Mak-Jurkauskas, M. Belenky, J. Herzfeld and R. G. Griffin, *Proc. Natl. Acad. Sci. U. S. A.*, 2009, **106**, 9244.
15 M. L. Mak-Jurkauskas, V. S. Bajaj, M. K. Hornstein, M. Belenky, R. G. Griffin and J. Herzfeld, *Proc. Natl. Acad. Sci. U. S. A.*, 2008, **105**, 883.
16 P. C. A. van der Wel, K. N. Hu, J. Lewandowski and R. G. Griffin, *J. Am. Chem. Soc.*, 2006, **128**, 10840.
17 R. Nelson, M. R. Saway, M. Balbirnie, A. O. Madsen, C. Riekel, R. Grothe and D. Eisenberg, *Nature*, 2005, **435**, 773.
18 M. R. Sawaya, S. Sambashivan, R. Nelson, M. I. Ivanova, S. A. Sievers, M. I. Apostol, M. J. Thompson, M. Balbirnie, J. J. W. Wiltzius, H. T. McFarlane, A. O. Madsen, C. Riekel and D. Eisenberg, *Nature*, 2007, **447**, 453.
19 P. C. A. van der Wel, J. Lewandoswki and R. G. Griffin, *J. Am. Chem. Soc.*, 2007, **129**, 5117.
20 N. M. Szeverenyi, M. J. Sullivan and G. E. Maciel, *J. Magn. Reson.*, 1982, **47**, 462.
21 A. W. Hing, S. Vega and J. Schaefer, *J. Magn. Reson.*, 1992, **96**, 205.
22 C. P. Jaroniec, C. Filip and R. G. Griffin, *J. Am. Chem. Soc.*, 2002, **124**, 10728.
23 M. Balbirnie, R. Grothe and D. S. Eisenberg, *Proc. Natl. Acad. Sci. U. S. A.*, 2001, **98**, 2375.
24 C. R. Morcombe and K. W. Zilm, *J. Magn. Reson.*, 2003, **162**, 479.
25 J. L. Markley, A. Bax, Y. Arata, C. W. Hilbers, R. Kaptein, B. D. Sykes, P. E. Wright and K. Wuthrich, *J. Mol. Biol.*, 1998, **280**, 933.
26 R. K. Harris, E. D. Becker, S. M. C. de Menezes, R. Goodfellow and P. Granger, *Solid State Nucl. Magn. Reson.*, 2002, **22**, 458.
27 A. B. Barnes, B. Corzilius, M. L. Mak-Jurkauskas, L. B. Andreas, V. S. Bajaj, Y. Matsuki, M. L. Belenky, J. Lugtenburg, J. R. Sirigiri, R. J. Temkin, J. Herzfeld and R. G. Griffin, *Phys. Chem. Chem. Phys.*, 2010, **12**, DOI: 10.1039/c003763j.
28 K. N. Hu, V. S. Bajaj, M. Rosay and R. G. Griffin, *J. Chem. Phys.*, 2007, **126**, 044512.
29 E. F. Pettersen, T. D. Goddard, C. C. Huang, G. S. Couch, D. M. Greenblatt, E. C. Meng and T. E. Ferrin, *J. Comput. Chem.*, 2004, **25**, 1605.
30 P. C. A. van der Wel, J. Lewandoswki and R. G. Griffin, *Biochemistry*, 2010, submitted.
31 T. G. Pedersen, B. W. Sigurskjold, K. V. Andersen, M. Kjaer, F. M. Poulsen, C. M. Dobson and C. Redfield, *J. Mol. Biol.*, 1991, **218**, 413.
32 V. Chevelkov, K. Faelber, A. Diehl, U. Heinemann, H. Oschkinat and B. Reif, *J. Biomol. NMR*, 2005, **31**, 295.

5918 | *Phys. Chem. Chem. Phys.*, 2010, **12**, 5911–5919

This journal is © the Owner Societies 2010

33 A. Lesage and A. Bockmann, *J. Am. Chem. Soc.*, 2003, **125**, 13336.
34 W. Gallagher, F. Tao and C. Woodward, *Biochemistry*, 1992, **31**, 4673.
35 E. K. Paulson, C. R. Morcombe, V. Gaponenko, B. Dancheck, R. A. Byrd and K. W. Zilm, *J. Am. Chem. Soc.*, 2003, **125**, 14222.
36 A. Lesage, L. Emsley, F. Penin and A. Bockmann, *J. Am. Chem. Soc.*, 2006, **128**, 8246.
37 R. Kempkes, E. Stofko, K. Lam and E. H. Snell, *Acta Crystallogr., Sect. D: Biol. Crystallogr.*, 2008, **64**, 287.
38 J. L. Dashnau, N. V. Nucci, K. A. Sharp and J. M. Vanderkooi, *J. Phys. Chem. B*, 2006, **110**, 13670.

This journal is © the Owner Societies 2010

Phys. Chem. Chem. Phys., 2010, **12**, 5911–5919 | 5919